Characterization of Cr Doped CuGaS2 Thin Films Synthesized By Chemical Spray Pyrolysis

N Ahsan, S Kalainathan, N Miyashita, T Hoshii, Y Okada

▶ **To cite this version:**

N Ahsan, S Kalainathan, N Miyashita, T Hoshii, Y Okada. Characterization of Cr Doped CuGaS2 Thin Films Synthesized By Chemical Spray Pyrolysis. Mechanics, Materials Science & Engineering MMSE Journal. Open Access, 2017, 9, 10.2412/mmse.53.55.304 . hal-01504783

HAL Id: hal-01504783
https://hal.science/hal-01504783

Submitted on 10 Apr 2017

HAL is a multi-disciplinary open access archive for the deposit and dissemination of scientific research documents, whether they are published or not. The documents may come from teaching and research institutions in France or abroad, or from public or private research centers.

L'archive ouverte pluridisciplinaire **HAL**, est destinée au dépôt et à la diffusion de documents scientifiques de niveau recherche, publiés ou non, émanant des établissements d'enseignement et de recherche français ou étrangers, des laboratoires publics ou privés.

Distributed under a Creative Commons Attribution 4.0 International License

Characterization of Cr Doped $CuGaS_2$ Thin Films Synthesized By Chemical Spray Pyrolysis

N. Ahsan[1,a], S. Kalainathan[1,2], N. Miyashita[1], T. Hoshii[3], Y. Okada[1]

1 – Research Center for Advanced Science and Technology (RCAST), The University of Tokyo, Japan

2 – Centre for Crystal Growth, VIT University, Vellore, India

3 – School of Engineering, Tokyo Institute of Technology, Tokyo, Japan

a – ahsan@mbe.rcast.u-tokyo.ac.jp

DOI **10.2412/mmse.53.55.304** provided by Seo4U.link

Keywords: density functional theory, thin films, intermediate band solar cells, spray pyrolysis, $CuGaS_2$.

ABSTRACT. Addition of an impurity or intermediate band in a semiconductor can extend its optical functionalities to novel application such as intermediate band solar cells (BSCs). For this purpose, the optical and electronic characterization were performed on Chromium (Cr) doped (1-4%) chalcopyrite $CuGaS_2$ (CGS) thin films synthesized by chemical spray pyrolysis technique on glass substrates. The structural and chemical characterization studied in the past confirmed that the prepared films are in tetragonal chalcopyrite structure with polycrystalline nature [1]. In the present study, electronic transitions studied by photo-modulated reflectance (PR) measurements showed widened bandgaps when Cr was added, and agrees well with our calculation based on density functional theory (DFT). Native defect-related transitions typically observed within the bandgap of the host CGS semiconductor were reduced in the Cr added films. This observation is consistent with photo-luminescence (PL) spectra measured at room temperature. An additional signature of an impurity band emerged in the PR transitions for Cr-added samples. Analysis of spin-resolved density of state calculation suggests that the IB originates from spin-polarized bands.

Introduction. Addition of an intermediate band (IB) such as an impurity band can extend the functional limit posed by the conventional two-band character of semiconductor materials. For example, the concept of intermediate band solar cells (IBSC) makes use of an intermediate step to excite electrons from the valence band (VB) to the conduction band (CB) by two-step photon absorption (TSPA) of long wave-length photons that otherwise transpire through the material [2]. Detailed balance calculation predicts conversion efficiency of 65.1% for a three band solar cell (e.g. VB, IB, CB) under maximal solar concentration which is much higher than the conventional solar cell consisting two bands (e.g. VB and CB) [3]. The key operational demonstration of TSPA both at low [4] and room temperature [5-7] has been presented in a few IB systems of thin films and nanostructures despite much enhancement is needed in the magnitude of the TSPA driven current for practical application.

The quest for three band system have been spanned over various IB materials in recent years such as thin films of highly mismatched alloy (HMA) III-V dilute nitrides and II-VI oxides [5,8-10], deep impurity doped hosts [6], and nanostructures using quantum dots [11], quantum rings [12], etc. Key factors that drive IB formation process are different in each approach, and consist of host electronic structures, structural dimensionality, nature of the impurity atoms, etc. In HMA thin films, isoelectric impurities atoms with much different affinity and size in III-V and II-VI hosts modifies electronic structures remarkably with distinct three band features [13-15]. Low-dimensional structures such as QD array produce distinct mini-bands due to quantum-size effect [2]. Fabrication of large number in density and stacks of QD array can promote the needed optical absorption for IR-generated currents. In order to improve the IBSC efficiency, host materials with much wider band gap such as AlGaAs or InGaP are required [16].

For solar cells, Cu-based chalcopyrite semiconductors attract research interests mainly due to their higher absorption coefficients suitable for thin-film application. Of particular, the direct bandgap of $CuGaS_2$ or 'CGS' in short lies in the green region of the visible spectrum at room temperature [17]. It can be a suitable IB host since its bandgap of 2.4eV is relatively wide, and can accommodate impurity or IB bands sufficiently deep to avoid thermal escape of photo-generated carriers staying at the IB bands. Doping of transition metals in CGS has been predicted to be a potential candidate for IB solar cells [18]. Earlier reports for doping of transition metals such as Fe [19], V [20], Mn [21], Cr [22], Zn, Ti [23] to the CGS hosts have been predicted for the creation of IB. The valency match and the less distortion in lattice make the transition and rare earth elements to a suitable dopant for a chalcopyrite lattice.

Recently, we have reported that chemical spray pyrolysis deposition technique can be employed fabricating Cr doped CGS thin films on glass substrates maintaining polycrystalline qualities [1]. The addition of chromium didn't produce any observable lattice changes in X-ray diffraction, presumably due to similar ionic radii and electron affinity. The pyrolysis technique is employed to extend its application to cost effective large scale production. In this paper, at first, we study the optical properties using photo-modulated reflectance (PR) and photoluminescence (PL) characterizations at room temperature. Next, electronic band structure and density of state analysis are performed based on density functional theory (DFT). Sub-bandgap transitions in PR and modification in PL in Cr added CGS thin films have been discussed in terms of the calculation.

Experimental. Thin films were synthesized by chemical spray pyrolysis technique on glass substrates. The precursor solution for the host CGS synthesis consists 0.1 M of copper acetate, gallium chloride and of thiourea dissolved in deionised water. For Cr doping, the molar concentration of chromium chloride was varied between (1-4 wt%). The follow-on mixture solution was deposited on glass substrates by the chemical spray pyrolysis technique. Temperature of the glass substrates was maintained at 250 $^{\circ}$C. Obtained thin films thickness is in the range of ~ 2 □m. The thin films were single phase as confirmed by X-ray diffraction, and presence of Cr ions were characterized by X-ray photoelectron spectroscopy. Details of the synthesis and physical characterization is published elsewhere [1].

Photo-modulated reflectance (PR) spectroscopy was performed at room temperature utilizing a mechanically chopped 405 nm line of a 15 mW solid-state laser. The applied laser intensity for PR measurements was kept constant at 33 mW/cm^2. Details of the PR system is explained elsewhere [6]. Photo-luminescence (PL) spectroscopy was performed at room temperature utilizing 405 nm line of a 30 mW solid-state laser. In order to improve the PL signals by suppressing wave-guiding effect of the glass substrate, PL signal collection was made under total reflection condition monitored by reflectivity from glass in a secondary photo detector. The electronic structures were calculated based on density functional theory (DFT) of siesta code using GGA exchange-correlation functionals [24].

Photo-modulated reflectance (PR) characterization. PR spectra of the samples are shown in Figs. 1. The structures in the high energy regions are related to the host bandgap E_g (VB→CB) transitions. The E_g values and width (Γ) od the transitions were retrieved using a third derivative low electric field model [25], which are 2.47 eV and 0.22eV for the present CGS film without Cr addition. The E_g and Γ values are 2.87 eV and 0.03 eV for 1% Cr, and 2.87 and 0.09 eV for 4% Cr-added samples, respectively. The high width values Γ indicate the presence of compostional and spatial inhomogeniety in the thin films. On the other hand, Cr addition extend the bandgaps of the host material from 2.47 eV to 2.87 eV. The long tails below the bandgaps are commonly observed in materials when compsitional inhomogeneity is promiment. Inside the host bandgap, as shown in Fig. 1(a), there appears two addtional transitons E_{D1} and E_{D2} involving defect bands of CGS native defects. With Cr addtion, transiton strength of both of the defect bands in Fig. 1(b) are much suppressed. This leads to an overall improvement of the PR background in the bandgap region, and observation of PR transitons E_{IB} below the E_g location in the Cr added thin films in Fig. 1(b). This transiton feature

(VB→IB) indicates the emergence of an impurity band (IB) inside the gap. The energy position E_{IB} is around 2.25 eV.

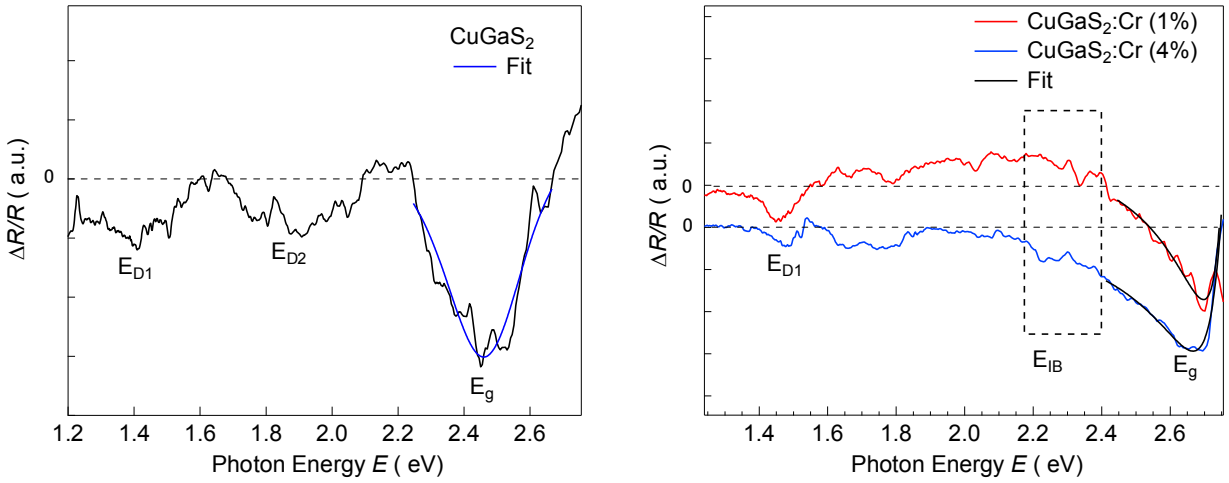

Fig 1. Room temperature PR spectra of $CuGaS_2$ thin films without and with Cr impurities. PR features are assigned to two native defects E_{D1} and E_{D2} at low energy region, and an impurity bands E_{IB} and bandgaps E_g at high energy region. Least squares fits are drawn for the bandgaps.

Photoluminescence (PL) studies. Fig. 2 shows the PL spectra for CGS thin films with different level of Cr dopants. The sharp line at about 1.53 eV is grating-scattered light of the diode-pumped laser (405 nm or 3.06 eV). Another narrow peak at 1.91 eV also originates from the scattered light. Although in standard case optical filters are set to cancel scattered light out, such a measure was not taken in the present experiments in order to allow PL detection from hosts' high bandgaps. At low energy region, the 1.53 eV line overlapped with a native defect peak, assigned E_{D1} in PR, and only faintly observed in the CGS without Cr. In the mid energy region, the broad and strong PL peak at the energy around 1.8 eV matches well with the PR assigned peak E_{D2}. This PL signals, in accordance with past reports on MOVPE grown samples [26], can be attributed to a defect band due to low Cu/Ga ratios (<0.84). A similar band is also observed in thin films produced under S-poor conditions, and annealing under S-overpressure has been shown effective to remove the defects [27]. In the present spectra, the E_{D2} locations are nearly constant with minor red-shifts by around 20 meV in the Cr added samples. The PL intensities of the defect bands are observed reduced with increasing Cr in consistent with a similar trend in PR transition strengths of the defects, and can be attributed to a partial passivation of the native defects due to Cr addition. At the high energy region in Fig. 3, weak PL signals can be observed at around 2.33 eV for the CGS thin film without Cr, and nearly matches with PR assigned E_g peak although around 100 meV away at 2.43 eV. This slight difference can be ascribed to the presence of long low-energy tails observed in PR. Past report show that PL signals often are generated from tail states where strong photo-carrier trapping and re-trapping occur, and give rise to S-shape behaviour in temperature-dependent PL peak traces [28]. An improvement in material homogeneity can reduce this gap. The Cr-added samples did not produce E_g related PL at photon energy up to 2.6 eV beyond which the direct beam of excitation laser affects PL background significantly, and perhaps buries the E_g signals of Cr added samples underneath.

The inset of Fig. 2 shows the enlargement of the PL magnitude at the high energy region in which response from the IB band expected. Weak peaks can be observed for the Cr added samples nearly at the host E_g location. Since PR analysis also suggests about the presence of the E_{IB} nearby, it is difficult to differentiate the assignment of the peaks.

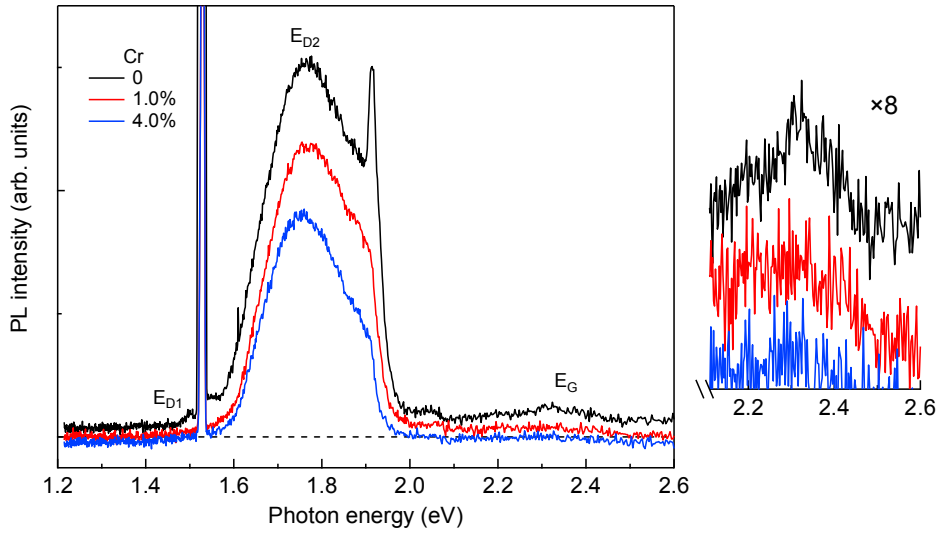

Fig.2. Room-temperature PL spectra for the thin films with different Cr contents. PL peaks are assigned to transitions two native defects E_{D1} and E_{D2} at low energy region, and bandgaps E_g at high energy regions.

The inset 2 shows the enlargement of the PL magnitude between 2.2 – 2.6 eV in which response from the IB band expected.

Band structure analysis. In order to analyse the electronic structure, band structures were calculated by first principles theoretical calculations based on density functional theory (DFT). The 2×2×1 super-cell considered in the present work is a 64-atom system consisting four units of conventional 16-atom chalcopyrite tetragonal cells stacked along the x- and y-axes. The corresponding symmetry of the super-cell is the space group 81: $P\bar{4}$. In the supercell, one Ga atom was replaced with the Cr atom accounting to the impurity concentration is about 1.56% in total, and 6.25% in Ga sites (or, x = 0.0625). This value is comparable to that used in the present experiments.

Calculations have been performed with the SIESTA code [24], an ab initio periodic density-functional method, self-consistent in the local density approximation. Norm-conserving, nonlocal pseudopotentials and linear combination of atomic orbitals have been used. The exchange-correlation effects of the valence electrons were described through the generalized gradient approximation (GGA), within the Perdew-Burke-Ernzerhof (PBE) functional. The Monkhorst-Pack scheme was set 6×6×6 for the pure case, and 3×3×3 for the doping cases for Brillouin zone sampling. In order to get accurate results, we optimized atomic coordinates, which were obtained by minimizing the total energy and atomic forces. The relaxation run was considered converged when the force on the atom was less than 0.04 eV/Å. Before relaxation, experimental values of CGS lattice constants were set, a=5.3512 Å and c/2a=0.98 [29]. Then we calculated the electronic structures for each optimized model.

Fig. 3 show the band structures along the high symmetrical directions of the Brillouin zone for the CGS and Cr doped crystals. As observed, the band structure of Cr-doped CGS is nearly same to the non-doped one, except that the band-gap is widened and an intermediate band appears in the bandgap. More importantly, the Fermi level exists inside the intermediate band. This suggests that the IB band is partially filled, which is a key requirement in order to realize an operational IBSC via TSPA process. The lowest band gap between the VB and CB is located at Γ point, and it's a direct bandgap with a value of 0.64 eV for the non-doped and 0.88 for the Cr-doped crystals. Although experimental values of our CGS is around 2.4 eV [1], such an underestimation of the calculated bandgaps is an inherent feature of the DFT method.

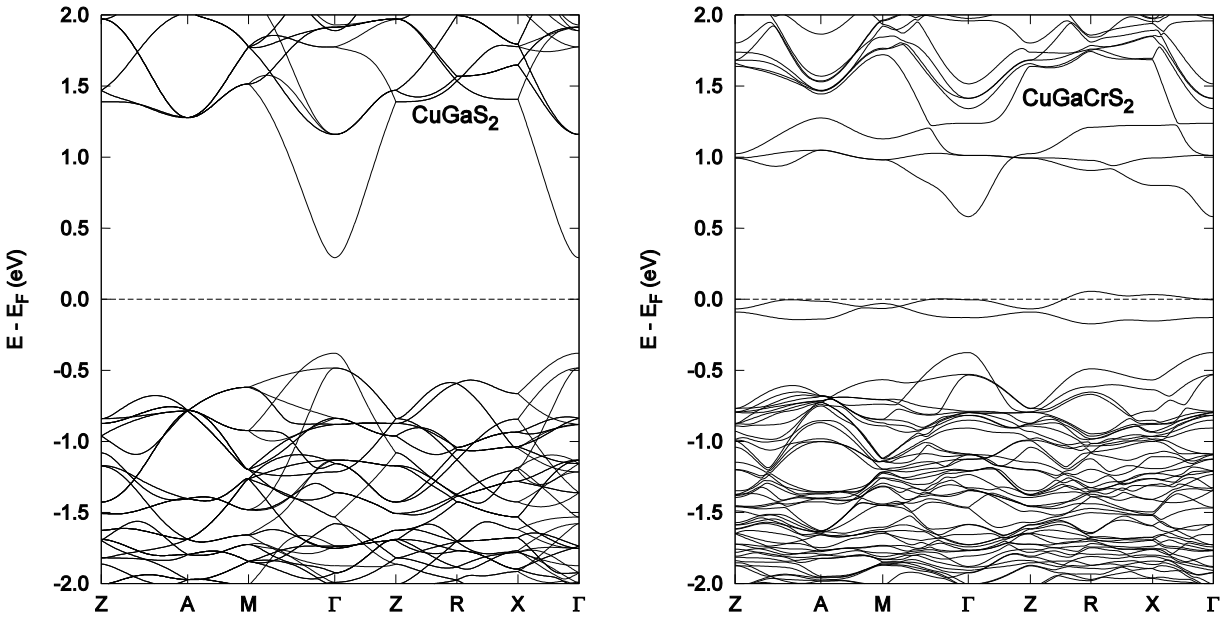

Fig 3. The bulk electronic band structure for CuGaS2 (left) and CuGaCrS2 (right) in the DZ-GGA calculations after dynamical relaxation. Spin orientation was set random. The Fermi level of the compound has been set at the energy zero. The diagram is displayed in the main directions of the corresponding first Brillouin zone.

Density of states analysis (DOS). The IB band was confirmed by analysing the DOS of the Cr doped CGS. Spin resolved total density of states (DOS) over all atomic orbitals are shown in Fig. 4. The Fermi level has been set at the energy zero. The partially filled IB mainly contains up-spin states while the down spin states maintains the conventional two-band character. These situations fulfil a key requirement in order to realize efficient two-step photon absorption (TSPA) process.

There is another spin-band around 0.40 eV below the conduction band (CB). The PR retrieved E_{IB} location is of similar order deeper from the CB, and can be ascribed to the spin-band in Fig. 4. However, further verification is needed to confirm the origin. Because a wide separation of the IB band can limit the thermal excitation of IB electrons and can promote photo-excitation via TSPA, this upper IB band can be made optically active for TSPA if suitable filling of the band can be designed.

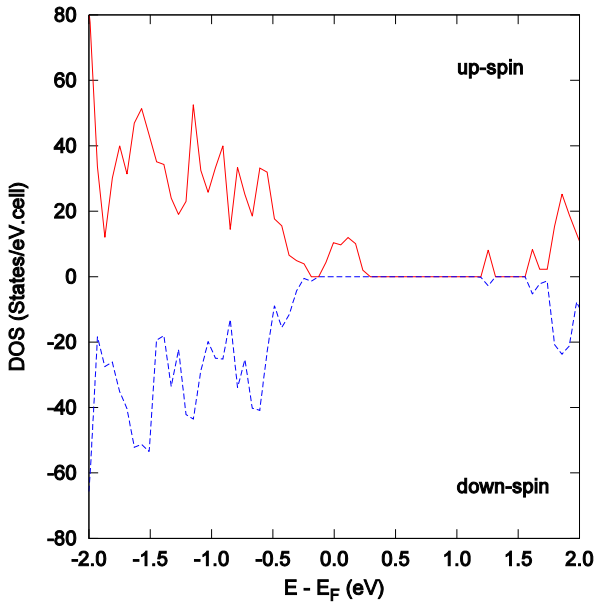

Fig 4. Spin resolved total density of states (DOS) over all atomic orbitals in $CuGaS_2$ with Cr doping. The Fermi level has been set at the energy zero.

Summary. The key finding of the present study is the observation of sub-band gap optical response for Cr doped CGS thin films, and its assignment to an intermediate band by means of theoretical band structure evolution.

Acknowledgement. This work is supported by New Energy and Industrial Technology Development Organization (NEDO), and Ministry of Economy, Trade and Industry (METI), Japan. Parts of this work was performed under the JSPS fellowship for research program in Japan, and supported by Hirose International Scholarship Foundation, Japan.

References

[1] S. Kalainathan, N. Ahsan, T. Hoshii, and Y. Okada, "Tailoring of Intermediate Band in CuGaS2 Thin film via Chromium doping by facile chemical Spray Pyrolysis technique," *Materials Science in Semiconductor Processing,* vol. submitted.

[2] Y. Okada, N. J. Ekins-Daukes, T. Kita, R. Tamaki, M. Yoshida, A. Pusch*, et al.*, "Intermediate band solar cells: Recent progress and future directions," *Applied Physics Reviews,* vol. 2, p. 021302, 2015.

[3] A. Luque and A. Martí, "Increasing the Efficiency of Ideal Solar Cells by Photon Induced Transitions at Intermediate Levels," *Phys. Rev. Lett.,* vol. 78, pp. 5014-5017, 1997.

[4] A. Martı´, E. Antolı´n, C. R. Stanley, C. D. Farmer, N. Lo´pez, P. Dı´az*, et al.*, "Production of Photocurrent due to Intermediate-to-Conduction-Band Transitions: A Demonstration of a Key Operating Principle of the Intermediate-Band Solar Cell," *Phys. Rev. Lett.,* vol. 97, p. 247701, 2006.

[5] N. Ahsan, N. Miyashita, M. M. Islam, K. M. Yu, W. Walukiewicz, and Y. Okada, "Two-photon excitation in an intermediate band solar cell structure," *Appl. Phys. Lett.,* vol. 100, p. 172111, 2012.

[6] N. Ahsan, N. Miyashita, M. M. Islam, K. M. Yu, W. Walukiewicz, and Y. Okada, "Effect of Sb on GaNAs Intermediate Band Solar Cells," *IEEE J. Photovolt.,* vol. 3, pp. 730-736, 2013.

[7] Y. Okada, T. Morioka, K. Yoshida, R. Oshima, Y. Shoji, T. Inoue*, et al.*, "Increase in photocurrent by optical transitions via intermediate quantum states in direct-doped InAs/GaNAs strain-compensated quantum dot solar cell," *Journal of Applied Physics,* vol. 109, p. 024301, 2011.

[8] T. Tanaka, K. M. Yu, A. Levander, O. Dubon, L. Reichertz, N. Lopez, *et al.*, "Demonstration of ZnTe1-xOx Intermediate Band Solar Cell," *Jpn. J. Appl. Phys.,* vol. 50, p. 082304, 2011.

[9] T. Tanaka, M. Miyabara, Y. Nagao, K. Saito, Q. Guo, M. Nishio, *et al.*, "Photogenerated Current By Two-Step Photon Excitation in ZnTeO Intermediate Band Solar Cells with n-ZnO Window Layer," *IEEE J. Photovolt.,* vol. 4, p. 196, 2014.

[10] N. Lo´pez, L. A. Reichertz, K. M. Yu, K. Campman, and W. Walukiewicz, "Engineering the Electronic Band Structure for Multiband Solar Cells," *Phys. Rev. Lett.,* vol. 106, p. 028701, 2011.

[11] R. Oshima, A. Takata, and Y. Okada, "Strain-compensated InAs/GaNAs quantum dots for use in high-efficiency solar cells," *Appl. Phys. Lett.,* vol. 93, p. 083111, 2008.

[12] J. Wu, D. Shao, Z. Li, M. O. Manasreh, V. P. Kunets, Z. M. Wang, *et al.*, "Intermediate-band material based on GaAs quantum rings for solar cells," *Appl. Phys. Lett.,* vol. 95, p. 071908, 2009.

[13] W. Walukiewicz, W. Shan, K. M. Yu, J. W. A. III, E. E. Haller, I. Miotkowski, *et al.*, "Interaction of Localized Electronic States with the Conduction Band: Band Anticrossing in II-VI Semiconductor Ternaries," *Phys. Rev. Lett.,* vol. 85, p. 1552, 2000.

[14] J. Wu, W. Walukiewicz, K. M. Yu, J. W. Ager, E. E. Haller, I. Miotkowski, *et al.*, "Origin of the large band-gap bowing in highly mismatched semiconductor alloys," *Phys. Rev. B,* vol. 67, p. 035207, 2003.

[15] W. Shan, K. M. Yu, W. Walukiewicz, J. Wu, J. W. A. III, and E. E. Haller, "Band anticrossing in dilute nitrides," *J. Phys.: Cond. Mat.,* vol. 16, p. S3355, 2004.

[16] Y. Dai, M. A. Slocum, Z. Bittner, S. Hellstroem, D. V. Forbes, and S. M. Hubbard, "Optimization in wide-band-gap quantum dot solar cells," *43rd IEEE Photovoltaic Specialists Conference (PVSC),* pp. 0151 - 0154, 2016.

[17] W.-J. Jeong and G.-C. Park, "Structural and electrical properties of CuGaS2 thin films by electron beam evaporation," *Solar Energy Materials & Solar Cells,* vol. 75, pp. 93 –100, 2003.

[18] A. Martí, D. F. Marrón, and A. Luque, "Evaluation of the efficiency potential of intermediate band solar cells based on thin-film chalcopyrite materials," *J. Appl. Phys.,* vol. 103, p. 073706, 2008.

[19] K. Sato and T. Teranishi, "Effect of Delocalization of d-Electrons on the Optical Reflectivity Spectra of $CuGa_{1-x}Fe_xS_2$ and $CuAl_{1-x}Fe_xS_2$ Systems," *Jpn. J. Appl. Phys.,* vol. 19, pp. 101 - 105, 1980.

[20] P. Palacios, K. Sánchez, J. C. Conesa, J. J. Fernández, and P. Wahnón, "Theoretical modelling of intermediate band solar cell materials based on metal-doped chalcopyrite compounds," *Thin Solid Films,* vol. 515, pp. 6280 –6284, 2007.

[21] Y.-J. Zhao and A. Zunger, "Electronic structure and ferromagnetism of Mn-substituted $CuAlS_2$, $CuGaS_2$, $CuInS_2$, $CuGaSe_2$, and $CuGaTe_2$," *Phys. Rev. B,* vol. 69, p. 104422, 2004.

[22] P. Palacios, I. Aguilera, P. Wahnón, and J. C. Conesa, "Thermodynamics of the Formation of Ti- and Cr-doped $CuGaS_2$ Intermediate-band Photovoltaic Materials," *J. Phys. Chem. C,* vol. 112, pp. 9525 - 9529, 2008.

[23] Y. Seminóvski, P. Palacios, and P. Wahnón, "Intermediate band position modulated by Zn addition in Ti doped $CuGaS_2$," *Thin Solid Films,* vol. 519, pp. 7517 - 7521, 2011.

[24] J. M. Soler, E. Artacho, J. D. Gale, A. García, J. Junquera, P. Ordejón, *et al.*, "The SIESTA method for ab initio order-N materials simulation," *Journal of Physics: Condensed Matter,* vol. 14, p. 2745, 2002.

[25] D. E. Aspnes, "Third-derivative modulation spectroscopy with low-field electroreflectance," *Surf. Sci.,* vol. 37, pp. 418–442, 1973.

[26] J. R. Botha, M. S. Branch, P. R. Berndt, A. W. R. Leitch, and J. Weber, "Defect chemistry in CuGaS2 thin films: A photoluminescence study," *Thin Solid Films,* vol. 515, pp. 6246-6251, 2007.

[27] G. Massé, "Luminescence of $CuGaS_2$," *J. Appl. Phys.,* vol. 58, pp. 930 - 935, 1985.

[28] N. Ahsan, N. Miyashita, K. M. Yu, W. Walukiewicz, and Y. Okada, "Improving multiband character of GaNAs," *Submitted*.

[29] A. H. Romero, M. Cardona, R. K. Kremer, R. Lauck, G. Siegle, C. Hoch, *et al.*, "Electronic and phononic properties of the chalcopyrite $CuGaS_2$," *Phys. Rev. B,* vol. 83, p. 195208, 2011.

Cite the paper

N. Ahsan, S. Kalainathan, N. Miyashita, T. Hoshii, Y. Okada (2017). Characterization of Cr Doped $CuGaS_2$ Thin Films Synthesized By Chemical Spray Pyrolysis. *Mechanics, Materials Science & Engineering*, Vol 9. doi:10.2412/mmse.53.55.304